

# Ab Initio Study on Adsorption of Hydrated Na<sup>+</sup> and Cu<sup>+</sup> Cations on the Cu(111) Surface

Antti J. Karttunen,<sup>†</sup> Richard L. Rowley,<sup>‡</sup> and Tapani A. Pakkanen<sup>\*,†</sup>

Department of Chemistry, University of Joensuu, P.O. Box 111, FI-80101, Joensuu, Finland, and Department of Chemical Engineering, Brigham Young University, Provo, Utah 84602

Received: August 3, 2005; In Final Form: October 28, 2005

The interactions of Na<sup>+</sup> and Cu<sup>+</sup> cations with a Cu(111) surface in the presence and absence of water molecules were investigated using cluster models and ab initio methods. Adsorption in aqueous solution was modeled with one to five water molecules around the adsorbing cation. The Cu surface was described with Cu<sub>10</sub> and Cu<sub>18</sub> cluster models and the computational method was MP2/RECP/6-31+G\*. The effect of the basis set superposition error (BSSE) was taken into account with counterpoise (CP) correction, and the accuracy of HF-level results was examined. The interactions between Na<sup>+</sup> and the Cu surface were found to be primarily electrostatic, and the energy differences among the different adsorption sites were small. The largest CP-corrected MP2 adsorption energy for the Cu<sub>18</sub> cluster was −188 kJ/mol. When water molecules were added around it, Na<sup>+</sup> receded from the Cu surface and finally was surrounded totally by the water molecules. The interactions between Cu<sup>+</sup> and the Cu surface were dominated by orbital interactions, and Cu<sup>+</sup> preferred to adsorb on sites where it could bind to more than one surface atom. The largest CP-corrected MP2 adsorption energy for the Cu<sub>18</sub> cluster was −447 kJ/mol. Adding water molecules around it did not cause Cu<sup>+</sup> to draw away from the surface, but instead the water molecules began to form hydrogen bonds with one another. The magnitude of BSSE was substantial in most cases. CP corrections did not, however, have a significant impact on the relative trends among the interaction energies.

## 1. Introduction

Copper is a widely used, nonferrous metal, with useful properties such as very high electrical conductivity and ease of galvanic precipitation.<sup>1</sup> An important industrial process utilizing copper is electrolytic deposition, where ions in aqueous solution are adsorbed on a surface to modify the properties of the surface material.<sup>2</sup> A thorough understanding of the mechanism of electrodeposition at the atomic level is necessary for efficient design and control of electrodeposition processes. The progress of an electrodeposition process can be examined at the atomic level with molecular dynamics simulations. For proper parametrization of the simulations, it is essential to be familiar with the interactions between the various elements of the electrodeposition process in aqueous solution (adsorbate, water molecules, and surface material). Despite the fundamental nature of these interactions, it is not clear how the water molecules affect the adsorption process and how the hydrated ionic adsorbates behave on a copper surface.

To obtain a clearer view of the behavior of ionic adsorbates in aqueous solution on a copper surface, we selected two sufficiently different adsorbates, Na<sup>+</sup> and Cu<sup>+</sup>. The gas-phase adsorption of Na on the copper surface has been studied previously but with Na as a neutral atom, not a Na<sup>+</sup> cation. Padilla-Campos et al.<sup>3</sup> examined the Na atom on a copper surface in their study on the adsorption of alkali metals on a Cu(111) surface. Similarly, for the adsorption of copper on metallic copper surface, previous studies have been conducted only for atomic Cu, not Cu<sup>+</sup>. Jacob et al.<sup>4</sup> used the B88/P86

density functional to investigate the gas-phase adsorption of the Cu atom on the (100) surface of copper.

In addition to the adsorbate–surface interactions, the interactions of water molecules with the adsorbing ions and copper surface play a key role in adsorption processes in aqueous solution. Na<sup>+</sup>(H<sub>2</sub>O)<sub>n</sub> complexes have been studied theoretically by Glendening and Feller,<sup>5,6</sup> Hashimoto and Morokuma,<sup>7</sup> and Bauschlicher et al.<sup>8</sup> An example of experimental studies on Na<sup>+</sup>-(H<sub>2</sub>O)<sub>n</sub> is the mass spectrometric investigation of Džidić and Kerbarle.<sup>9</sup> Theoretical research on Cu<sup>+</sup>(H<sub>2</sub>O)<sub>n</sub> complexes has been done by Feller et al.<sup>10</sup> and Bauschlicher et al.<sup>11</sup> As well, several mass spectrometric experimental studies have been carried out.<sup>12–14</sup> The interactions between water and the copper surface have been examined in a number of studies, one of the most recent being the MP2 study of water adsorption on cluster models of Cu(111) conducted by Ruuska et al.<sup>15</sup>

The present work investigates the interactions of Na<sup>+</sup> and Cu<sup>+</sup> with the Cu(111) surface in the presence and absence of water molecules. The effect of water molecules on the adsorption process was investigated by placing one to five water molecules around the adsorbing cation. The interaction energies for different adsorption sites were determined in the absence of water molecules. Optimal adsorbate geometries and interaction energies between the aqua complex and surface were calculated for hydrated adsorbates.

## 2. Theoretical Methods and Models

**2.1. Methods.** When a cationic adsorbate surrounded by water molecules approaches a copper surface, many interactions of a different magnitude affect the total energy of the system. The surface–adsorbate and adsorbate–water interactions are strong when compared with surface–water and water–water interac-

\* To whom correspondence should be addressed. E-mail: Tapani.Pakkanen@joensuu.fi.

<sup>†</sup> University of Joensuu.

<sup>‡</sup> Brigham Young University.

tions, but when an accurate description of the system is pursued, the weaker interactions cannot be neglected. Thus, an electron-correlated theoretical method is needed to thoroughly investigate the energetics of the surface–adsorbate–water systems. In addition, the effect of the basis set superposition error (BSSE) resulting from the finite size of the basis sets used in theoretical studies needs to be considered when the interaction energy between separate fragments is examined. Interaction of an adsorbate molecule and a surface is a typical case where BSSE contributions can be substantial.<sup>16</sup> BSSE is usually compensated for with use of the counterpoise (CP) correction,<sup>17</sup> although several studies have shown the CP method to overcorrect the interaction energies of small molecules.<sup>18,19</sup> For small systems, improving the basis set is a good way to decrease BSSE, but for larger systems, the size of the basis set cannot be expanded without a significant increase in computation costs. For large systems, therefore, the most efficient way to account for BSSE will usually be to apply the CP correction.

Different theoretical methods have been tested for  $\text{Cu}^+(\text{H}_2\text{O})_n$  and  $\text{Na}^+(\text{H}_2\text{O})_n$  complexes. Feller, Glendening, and de Jong<sup>10</sup> examined the  $\text{Cu}^+-\text{H}_2\text{O}$  interactions by several different methods and with several basis sets. Their smallest basis set for copper was the relativistic effective core potential (RECP) originally developed by Dolg et al.<sup>20</sup> and augmented by Feller et al. with a single set of *f*-type functions ( $\zeta_f = 2.7$ ).<sup>21</sup> In this RECP, the inner (1s, 2s, and 2p) orbitals of copper are replaced with a pseudopotential, and after addition of the *f*-functions, the outer shells are described with a contracted (8s, 7p, 6d, 1f)  $\rightarrow$  [6s, 5p, 3d, 1f] basis set. Six Cartesian *d*-functions and 10 Cartesian *f*-functions were used in all calculations with this basis set. The pseudopotential replaces 10 electrons, so a copper atom is left with 19 active electrons. A drawback of the use of *f*-functions within an ECP is that analytical gradients are no longer available in Gaussian03. Accounting for the relativistic effects in some way is important for copper, since Feller's group discovered that relativistic corrections are significant for some  $\text{Cu}^+(\text{H}_2\text{O})$  complexes. CP-corrected MP2 results with the RECP basis set for copper and 6-31+G\* basis set for water were in good agreement with results obtained with a high-level method (CCSD(T)) and very large, augmented correlation-consistent basis sets. MP2/RECP/6-31+G\* is thus a good combination for  $\text{Cu}^+(\text{H}_2\text{O})_n$  complexes, because the computational cost of MP2 is much less than that of more sophisticated correlated methods such as CCSD(T).

Glendening and co-workers<sup>5,6</sup> have investigated the  $\text{Na}^+(\text{H}_2\text{O})_n$  complexes in two different studies. The first study dealt with  $\text{M}^+(\text{H}_2\text{O})$  complexes with alkali metals ( $\text{M} = \text{Li}, \text{Na}, \text{K}, \text{Rb}, \text{and Cs}$ ), and the computational methods were MP2/6-31+G\* and RHF/6-31+G\*. The MP2/6-31+G\* results with CP correction for BSSE were found to compare favorably with the results from higher level methods and experimental measurements. Noncorrelated RHF/6-31+G\* also provided an adequate description of the complexes since cation–water interactions are principally electrostatic. In the second study, the same  $\text{M}^+(\text{H}_2\text{O})$  complexes were examined but with larger correlation-consistent basis sets. In comparison with higher level basis sets, MP2/6-31+G\* with CP correction for BSSE yielded reliable binding energies, although the geometries of the larger complexes were less well described. An interesting observation was that, for  $\text{M}^+(\text{H}_2\text{O})$  complexes, the inclusion of electron correlation had the smallest effect on  $\text{Na}^+(\text{H}_2\text{O})$  complexes.<sup>6</sup>

In view of the good performance of the MP2 method with the described RECP and 6-31+G\* basis sets in previous studies on  $\text{Cu}^+(\text{H}_2\text{O})_n$  and  $\text{Na}^+(\text{H}_2\text{O})_n$  complexes, we chose the MP2/

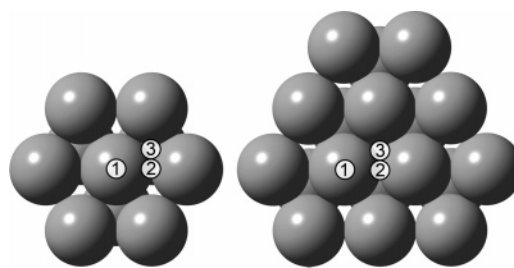


**Figure 1.** Top view of the  $\text{Cu}_{10}$  and  $\text{Cu}_{18}$  cluster models and three different adsorption sites: (1) on-top, (2) bridge, and (3) hollow.

RECP/6-31+G\* method for our study of the adsorption of  $\text{Cu}^+$  and  $\text{Na}^+$  in aqueous solutions. Since the size of our cluster models and the lack of analytical gradients would have made the geometry optimization of adsorbates very time-consuming with MP2, we first optimized all cation–water complexes adsorbed on the copper surface with Hartree–Fock and then calculated MP2 energies for the optimal HF geometries.

All calculated interaction energies in this work were treated with the counterpoise correction to reduce the effect of BSSE. Although the 6-31+G\* basis set used for  $\text{Na}^+$ , O, and H includes diffuse functions that should decrease BSSE to some degree, Glendening and Feller found CP-corrected results of the  $\text{Na}^+(\text{H}_2\text{O})$  complexes still to be closer to the experimental values than noncorrected results.<sup>5</sup> In their study on  $\text{Cu}^+(\text{H}_2\text{O})$  complexes, Feller et al.<sup>10</sup> found that the lack of tight *d*-functions on copper results in a significant BSSE contribution to the binding energies even when large basis sets are used.

All results presented in this study were calculated using the GAUSSIAN03, TURBOMOLE, and GAMESS quantum chemistry software packages.<sup>22–24</sup> TURBOMOLE was used to determine some adsorption energies with significantly larger clusters, and GAMESS was used in energy decomposition analysis. All the other results were obtained with GAUSSIAN.

**2.2. Models.** For fcc metals, such as copper, the most widely studied cleavage planes are the low-index (100), (110), and (111) planes. Of these, surface atoms are most tightly packed on the (111) plane, where every surface atom has nine coordinating neighbors. We chose to study the (111) cleavage plane described by two different-sized cluster models. Cluster models are the simplest way to model solid surfaces, and they can be used to describe the local aspects of surface chemistry, such as adsorbate–substrate interaction.<sup>25,26</sup> One drawback of the cluster approach is that the truncated coordination of the terminal atoms of the cluster may cause boundary effects. These tend to be especially troublesome for metal clusters because of the delocalized electron structure of metals.<sup>25,27</sup>

The cluster models used to describe the copper surface were  $\text{Cu}_{10}$  and  $\text{Cu}_{18}$  (Figure 1). Use of two different-sized clusters allows an investigation of the effect of cluster size on interaction energies. Both models have two atomic layers. The smaller  $\text{Cu}_{10}$  cluster has seven atoms in the surface layer and three atoms in the lower layer, while the larger  $\text{Cu}_{18}$  cluster has twelve atoms in the surface layer and six atoms in the lower layer. In both clusters, all atoms were described with the use of the full RECP described above. The experimental value 2.556 Å was used for the Cu–Cu distance.<sup>28</sup> The point group of both clusters is  $C_{3v}$ , so symmetry can be exploited to reduce the computational cost of the single-point calculations. All geometry optimizations of the adsorbates were performed without symmetry, and cluster atoms were always frozen in optimizations. Surface reconstruction was not taken into account because the reconstruction effect is usually negligible on transition metal surfaces.<sup>29,30</sup> The surface atoms on the closely packed (111) cleavage plane of copper

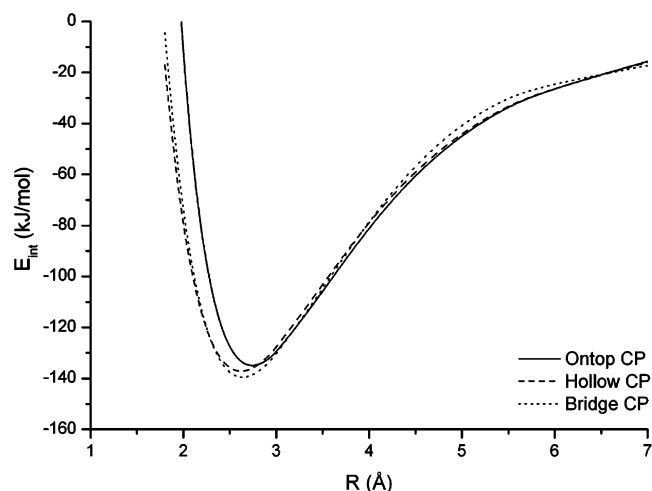


**Figure 2.** CP-corrected MP2 interaction energy curves for Na<sup>+</sup>–Cu<sub>10</sub> interaction at the on-top, bridge, and hollow adsorption sites.

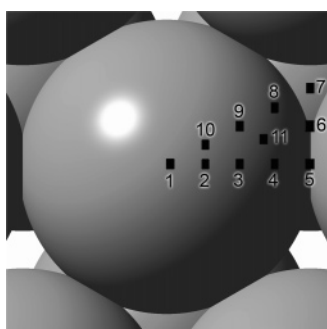


**Figure 3.** Location of the 11 Na<sup>+</sup> adsorption sites studied for the Cu<sub>10</sub> cluster. The atom in the picture is the center atom of the surface layer of the Cu<sub>10</sub> cluster. Point 1 represents the on-top site, point 5 the bridge site, and point 7 the hollow site.

also have a high coordination number, so there is little need for rearrangement to achieve a higher coordination of the atoms.<sup>27</sup>

The adsorption sites that were investigated are the on-top, bridge, and hollow sites normally considered for the (111) surfaces of copper. The locations of these adsorption sites on our cluster models are illustrated in Figure 1. The on-top site is always directly above a surface atom, the bridge site lies between two Cu atoms, and the hollow site is centered between three Cu atoms. With the larger Cu<sub>18</sub> cluster, all the adsorption sites are located on atoms that have proper coordination. With the Cu<sub>10</sub> cluster, only the on-top site is located on a surface atom with a coordination number of nine, the bridge and hollow sites are in contact with terminal atoms. For all three adsorption sites, the distance *R* between the adsorbate and the surface is always the orthogonal distance between the center of the adsorbate and the plane of surface copper centers.

### 3. Results and Discussion

**3.1. Adsorption of Na<sup>+</sup>.** The interaction energy curves for the interaction of Na<sup>+</sup> and the smaller Cu<sub>10</sub> cluster at the three adsorption sites are presented in Figure 2. The CP-corrected MP2 interaction energies for the three sites were closely similar in size. On the basis of this result, we decided to examine the Na<sup>+</sup>–Cu<sub>10</sub> interactions more closely and calculated the interaction energies for 11 different adsorption sites in total. The 11 adsorption sites are shown in Figure 3, and the corresponding MP2 interaction energies and equilibrium distances are listed in Table 1. The results in Table 1 demonstrate that the interaction

**TABLE 1: MP2 Results for the Na<sup>+</sup>–Cu<sub>10</sub> Interaction at 11 Adsorption Sites**

site	<i>R</i> <sub>eq</sub> <sup>a</sup> (Å)	<i>E</i> <sub>int</sub> <sup>b</sup> (kJ/mol)	<i>R</i> <sub>eq</sub> CP <sup>c</sup> (Å)	<i>E</i> <sub>int</sub> CP <sup>c</sup> (kJ/mol)	BSSE <sup>d</sup> (kJ/mol)	Δ <i>E</i> <sub>int</sub> CP <sup>e</sup> (kJ/mol)
1	2.66	−153.7	2.74	−135.2	18.5	5.7
2	2.65	−156.4	2.72	−137.6	18.8	3.3
3	2.62	−158.5	2.69	−139.8	18.7	1.1
4	2.59	−159.4	2.65	−140.9	18.5	0.0
5	2.58	−157.4	2.63	−139.8	17.6	1.1
6	2.56	−157.1	2.73	−138.9	18.1	2.0
7	2.55	−155.3	2.62	−137.5	17.8	3.4
8	2.56	−159.4	2.63	−140.4	19.0	0.5
9	2.61	−159.2	2.67	−140.2	19.0	0.7
10	2.64	−156.8	2.71	−138.0	18.8	2.9
11	2.59	−159.6	2.65	−140.6	18.9	0.3

<sup>a</sup> Equilibrium distance between Na<sup>+</sup> and the Cu surface. <sup>b</sup> Interaction energy at the equilibrium distance. <sup>c</sup> CP-corrected values of *R*<sub>eq</sub> and *E*<sub>int</sub>. <sup>d</sup> The difference between *E*<sub>int</sub> and *E*<sub>int</sub> CP. <sup>e</sup> The relative CP-corrected interaction energy of the site when the energy of the most favorable adsorption site is set to zero.

energies are closely similar regardless of the adsorption site and that the equilibrium distances are also almost identical. The largest CP-corrected MP2 interaction energy is −140.9 kJ/mol and the smallest −135.2 kJ/mol. Thus, the difference in interaction energies between the most favorable (4) and least favorable site (1) is only 5.7 kJ/mol. The flatness of the potential energy surface and the small variation of the equilibrium distances suggest that the interactions between the copper surface and Na<sup>+</sup> are mostly electrostatic and that Na<sup>+</sup> can move more or less freely on a copper surface at normal room temperature.

The magnitude of BSSE for the Na<sup>+</sup>–Cu<sub>10</sub> interaction energies is almost the same for the 11 adsorption sites, being 11–12% of the uncorrected energies. CP correction changes the most favorable site, as site 11 is the most favorable according to the uncorrected results, but after the CP correction, site 4 has the largest interaction energy. However, the difference in the interactions energies at these two sites is only 0.2 kJ/mol for the uncorrected and 0.3 kJ/mol for the CP-corrected energies making the change in the preference of the sites caused by BSSE irrelevant. Another notable result is the good performance of HF relative to MP2. The interaction energies obtained with HF were only 4–8% smaller than the CP-corrected MP2 results, and HF equilibrium distances (*R*) were only ca. 0.1 Å shorter than the corresponding MP2 distances. The difference in the HF and CP-corrected MP2 interaction energies varied among the adsorption sites and was largest for the on-top site. The electrostatic nature of Na<sup>+</sup>–Cu<sub>10</sub> interactions makes it possible to achieve results this accurate with an uncorrelated method like HF. The demonstrated usefulness of HF is important because, when studying the adsorption of Na<sup>+</sup>(H<sub>2</sub>O)<sub>*n*</sub>, the geometries of the Na<sup>+</sup>(H<sub>2</sub>O)<sub>*n*</sub> adsorbates on the copper surface are optimized with HF.

For the interaction between Na<sup>+</sup> and the larger Cu<sub>18</sub> cluster, the interaction energies were calculated only for on-top, bridge, and hollow sites. The MP2 interaction energies and equilibrium distances are shown in Table 2. For the Na<sup>+</sup>–Cu<sub>18</sub> interaction, the hollow site was the most favorable, with a CP-corrected interaction energy of −188.3 kJ/mol but the difference with the bridge site was only 3 kJ/mol (<2% of the total interaction energy). The on-top site was the least favorable adsorption site, with 15 kJ/mol smaller interaction energy than the hollow site (<9% of the total interaction energy). Compared with the results for the smaller cluster, the absolute values of the CP-corrected Na<sup>+</sup>–Cu<sub>18</sub> interaction energies are about one-third larger but the equilibrium distances diverge less than 0.1 Å from the Cu<sub>10</sub>



**TABLE 2: MP2 Results for the  $\text{Na}^+ - \text{Cu}_{18}$  Interaction at Three Different Adsorption Sites**

site <sup>a</sup>	$R_{\text{eq}}^b$ (Å)	$E_{\text{int}}^c$ (kJ/mol)	$R_{\text{eq}} \text{CP}^d$ (Å)	$E_{\text{int}} \text{CP}^d$ (kJ/mol)	BSSE <sup>e</sup> (kJ/mol)	$\Delta E_{\text{int}} \text{CP}^f$ (kJ/mol)
on-top (1)	2.65	−194.6	2.72	−173.5	21.2	14.8
bridge (5)	2.54	−210.8	2.60	−185.3	25.6	3.0
hollow (7)	2.55	−213.0	2.58	−188.3	24.8	0.0

<sup>a</sup> The number after the name of the adsorption site refers to the numbers used in Table 1. <sup>b</sup> Equilibrium distance between  $\text{Na}^+$  and the Cu surface. <sup>c</sup> Interaction energy at the equilibrium distance. <sup>d</sup> CP-corrected values of  $R_{\text{eq}}$  and  $E_{\text{int}}$ . <sup>e</sup> The difference between  $E_{\text{int}}$  and  $E_{\text{int}} \text{CP}$ . <sup>f</sup> The relative CP-corrected interaction energy of the site when the energy of the most favorable adsorption site is set to zero.

distances. The results for the  $\text{Na}^+ - \text{Cu}_{18}$  interaction support the conclusion that the interactions between the copper surface and  $\text{Na}^+$  are mostly electrostatic and the potential energy surface is flat. The magnitude of the BSSE for the  $\text{Na}^+ - \text{Cu}_{18}$  interaction energies is 11–12% of the uncorrected energies, which is identical with the result for the smaller cluster. CP correction does not change the order of magnitude of the interaction energies at different sites. As with the  $\text{Cu}_{10}$  cluster, the similarity of the HF and CP-corrected MP2 results is considerable. In contrast to the  $\text{Cu}_{10}$  cluster, the absolute values of the HF interaction energies are slightly larger than the CP-corrected MP2 energies. The difference in interaction energies is, however, very small: only 3.4 kJ/mol for the hollow site, 4.7 kJ/mol for the bridge site, and 12 kJ/mol for the on-top site. The corresponding differences in the equilibrium distance  $R_{\text{eq}}$  are 0.07, 0.07, and 0.03 Å. The relative difference in the interaction energy is only 2–7%.

Padilla-Campos et al.<sup>3</sup> studied the adsorption of metallic Na on the Cu(111) surface using a  $\text{Cu}_7$  cluster. They used Hartree–Fock and B88/P86 density functional combined with moderately sized basis sets. No corrections were made to account for BSSE. Their results showed the hollow site to be the most favorable adsorption site at the Hartree–Fock level and the on-top site at the DFT level. The HF interaction energy was −699.33 kJ/mol at the Na– $\text{Cu}_7$  distance of 2.40 Å, while the DFT interaction energy was −431.79 kJ/mol at the equilibrium distance of 2.60 Å. These energies are quite a bit larger than our interaction energies for  $\text{Na}^+$ . Padilla-Campos et al. concluded that both electrostatic and orbital contributions influence the interactions between the Na atom and the Cu surface. In the end, however, the adsorption energies were considered merely a starting point for more refined calculations, as there was some uncertainty in the results. The relatively small  $\text{Cu}_7$  cluster, where all the atoms are incompletely coordinated, probably caused some problems.

**3.2. Adsorption of  $\text{Na}^+(\text{H}_2\text{O})_n$ .** For the  $\text{Na}^+(\text{H}_2\text{O})_n$  complex, we examined the adsorption of complexes with one to five water molecules on the  $\text{Cu}_{10}$  cluster. As a first step, the geometry of the adsorbate complex on the  $\text{Cu}_{10}$  cluster was optimized at the Hartree–Fock level. Because the size of the  $\text{Cu}_{10}$  cluster is limited, some constraints had to be applied to the geometry optimizations to prevent adsorbates from binding to terminal surface atoms with deficient coordination.  $\text{Na}^+$  was allowed to move only perpendicularly to the surface, but no restrictions were placed on the water molecules. There were two types of initial geometries: one with  $\text{Na}^+$  closest to the surface and water molecules on top of  $\text{Na}^+$  and the other with all adsorbate molecules on the same plane. The initial geometry of the adsorbate had no effect on the final structure since the optimization algorithm was able to find the same optimal structure for different initial geometries. The final adsorbate geometries are shown in Figure 4. As the number of water

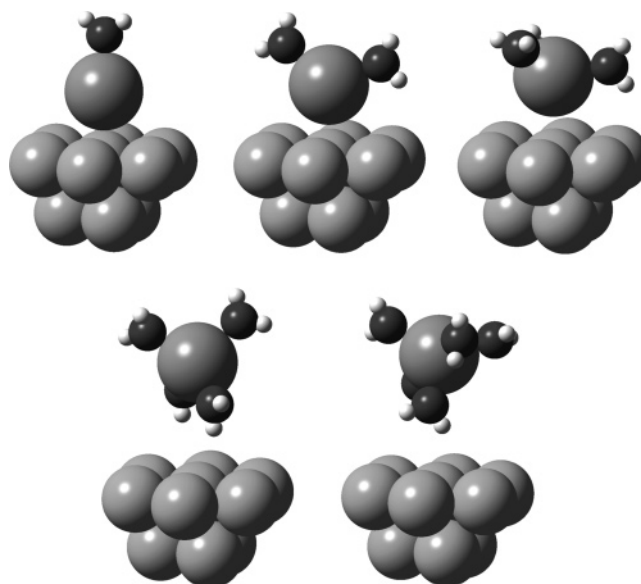


**Figure 4.** Optimized structures of the  $\text{Na}^+(\text{H}_2\text{O})_n$  complex for one to five water molecules adsorbed on the  $\text{Cu}_{10}$  cluster.  $\text{Na}^+$  was allowed to move only perpendicularly to the surface, but no restrictions were placed on the water molecules.  $\text{Na}^+ - \text{H}_2\text{O}$  distances were between 2.26 and 2.39 Å, the distance increasing with the number of water molecules.

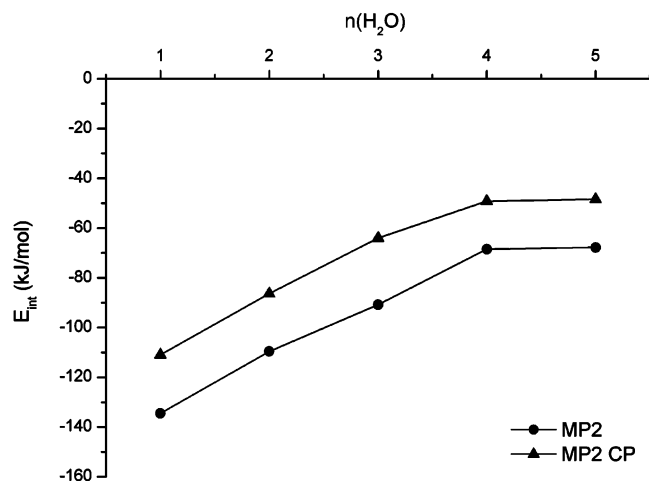
molecules around  $\text{Na}^+$  increases,  $\text{Na}^+$  is drawn away from the surface. When there are at least four water molecules around  $\text{Na}^+$ , it recedes from the surface far enough for two water molecules to move between it and  $\text{Cu}_{10}$ . To study this behavior more closely, we calculated MP2 energies for all HF-optimized structures. The MP2 energies and CP-corrected energies are shown in Table 3. The interaction energies  $E_{\text{int}}$  and  $E_{\text{int}} \text{CP}$  in Table 3 were obtained by subtracting the energies of the  $\text{Cu}_{10}$  cluster and the separately optimized  $\text{Na}^+(\text{H}_2\text{O})_n$  complex from the total energy of the  $\text{Na}^+(\text{H}_2\text{O})_n - \text{Cu}_{10}$  system. Thus, the calculated interaction energies include the (de)stabilization energy resulting from the changes in the optimal geometry of the separately optimized adsorbate complex when it is brought from infinite separation to the vicinity of the surface.

The  $E_{\text{int}} \text{CP}$  values in Table 3 show that the interaction energy between the  $\text{Na}^+(\text{H}_2\text{O})_n$  complex and  $\text{Cu}_{10}$  cluster decreases as the number of water molecules increases.  $\text{Na}^+$  interacts less with the cluster and recedes from the surface. When the number of water molecules increases from four to five, the value of  $E_{\text{int}} \text{CP}$  becomes almost constant. The change in the interaction energy is illustrated in Figure 5. When the water molecules move between  $\text{Na}^+$  and the surface, the interaction between  $\text{Na}^+$  and the surface weakens and the water–surface interactions become more important. To obtain an approximation of the interaction energy of a water molecule and the Cu surface, we performed a HF geometry optimization with the  $\text{Cu}_{10}$  cluster and a single water molecule. The water molecule was optimized without any constraints, and it ended up on the on-top site with hydrogens pointing toward the surface. The distance between the oxygen atom and the surface was 4.16 Å, and the CP-corrected MP2 interaction energy was −10.8 kJ/mol (the magnitude of the BSSE was 7.5 kJ/mol). In the study of Ruuska et al.,<sup>15</sup> the corresponding distance and interaction energy obtained from the CP-corrected MP2 potential energy curve were 3.62 Å and −12.4 kJ/mol. The difference in the results is probably due to a failure of the HF method to find the correct minimum geometry. The magnitude of the two interaction energies is more or less the same, however.

**TABLE 3: MP2 Results for Na<sup>+</sup>(H<sub>2</sub>O)<sub>n</sub>–Cu<sub>10</sub> Interaction**

<i>n</i>	<i>R</i> <sub>eq</sub> (Å)	<i>E</i> <sub>tot</sub> <sup>b</sup> (au)	<i>E</i> <sub>comp</sub> <sup>c</sup> (au)	<i>E</i> <sub>int</sub> <sup>d</sup> (kJ/mol)	<i>E</i> <sub>tot</sub> CP <sup>e</sup> (au)	<i>E</i> <sub>comp</sub> CP <sup>e</sup> (au)	<i>E</i> <sub>int</sub> CP <sup>e</sup> (kJ/mol)	BSSE <sup>f</sup> (kJ/mol)
1	2.88	−2205.9546	−237.9099	−134.5	−2205.9424	−237.9067	−110.9	23.6
2	3.05	−2282.1924	−314.1572	−109.6	−2282.1757	−314.1493	−86.3	23.3
3	3.38	−2358.4260	−390.3979	−90.8	−2358.4046	−390.3867	−64.0	26.8
4	5.24	−2434.6531	−466.6335	−68.5	−2434.6300	−466.6178	−49.2	19.4
5	5.54	−2510.8830	−542.8637	−67.8	−2510.8542	−542.8423	−48.4	19.4

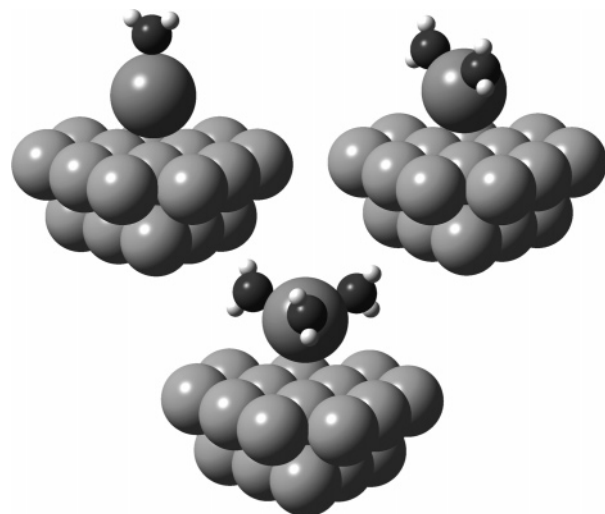
<sup>a</sup> Distance between Na<sup>+</sup> and the Cu surface at the optimum geometry. <sup>b</sup> Total energy of the Na<sup>+</sup>(H<sub>2</sub>O)<sub>n</sub>–Cu<sub>10</sub> system in hartrees. <sup>c</sup> Total energy of a separately optimized Na<sup>+</sup>(H<sub>2</sub>O)<sub>n</sub> complex in hartrees. <sup>d</sup> Interaction energy between Cu<sub>10</sub> and the Na<sup>+</sup>(H<sub>2</sub>O)<sub>n</sub> complex obtained from the expression  $E_{\text{int}} = (E_{\text{tot}} - E_{\text{comp}} + E(\text{Cu}_{10}))$ , where  $E(\text{Cu}_{10}) = -1967.9935$  au. <sup>e</sup> CP-corrected values of  $E_{\text{tot}}$ ,  $E_{\text{comp}}$ , and  $E_{\text{int}}$ . <sup>f</sup> Difference between  $E_{\text{int}}$  and  $E_{\text{int}}$  CP.

**Figure 5.** MP2 interaction energy and CP-corrected interaction energy between the Na<sup>+</sup>(H<sub>2</sub>O)<sub>n</sub> complex and Cu<sub>10</sub> cluster.

From the geometry optimizations and interaction energies obtained for the Na<sup>+</sup>(H<sub>2</sub>O)<sub>n</sub> complex on the Cu<sub>10</sub> cluster, it seems that, in aqueous solution, Na<sup>+</sup> will not adsorb directly on the surface but prefers to be surrounded by a shell of water molecules. Because both the Na<sup>+</sup>–Cu surface and Na<sup>+</sup>–H<sub>2</sub>O interactions are predominantly electrostatic, Na<sup>+</sup> has no preference for the surface if the alternative is to be completely surrounded by water molecules.

The absolute magnitude of the BSSE remains almost constant when the total interaction energy between the complex and surface decreases. As the number of water molecules increases, weak H<sub>2</sub>O–Cu<sub>10</sub> interactions become more important causing the relative magnitude of the BSSE to increase. Additionally, as the interactions become more complex, the HF interaction energies turn out to be less quantitative. In the case of one water molecule, the HF interaction energy ( $E_{\text{int}}$ ) is about 9% smaller than the corresponding CP-corrected MP2 energy ( $E_{\text{int}}$  CP), but as the number of water molecules increases, the difference becomes larger, being 33% for the case with five water molecules. Although the HF results are no longer quantitative, the qualitative trend seen in Figure 5 is reproduced with HF.

With the use of the larger Cu<sub>18</sub> cluster, the artificial geometrical restrictions on Na<sup>+</sup> can be discarded because the terminal effects have a smaller impact on the optimizations. The downside of the larger cluster model is that the optimizations become highly time-consuming because the different structural configurations of the water molecules are energetically very close to one another, and a long time is required for the optimization algorithm to find the real minimum. The lack of analytical gradients due to the combination of f-functions and an ECP basis adds to the difficulties in optimization. In view of the above, we examined only cases with one, two, and three water molecules. The final adsorbate geometries after the full Na<sup>+</sup>(H<sub>2</sub>O)<sub>n</sub> optimizations on Cu<sub>18</sub> are shown in Figure 6, and the MP2 energies are listed in Table 4. The Na<sup>+</sup>–Cu<sub>18</sub>

**Figure 6.** Optimized structures of the Na<sup>+</sup>(H<sub>2</sub>O)<sub>n</sub> complex adsorbed on the Cu<sub>18</sub> cluster for one to three water molecules. Na<sup>+</sup> and the water molecules were allowed to move freely on the surface. Na<sup>+</sup>–H<sub>2</sub>O distances were between 2.28 and 2.30 Å, the distance increasing with the number of water molecules.

equilibrium distances of the optimized structures show that Na<sup>+</sup> recedes from the surface in the same way as with the smaller cluster. When *n* increases from 1 to 2, Na<sup>+</sup> recedes 0.17 Å with both clusters, and as *n* grows to 3, the change in *R*<sub>eq</sub> is approximately 0.3 Å for both clusters. The absolute values of *R*<sub>eq</sub> are smaller for the larger cluster, however, because Na<sup>+</sup> is located on the hollow site instead of the on-top site. The interaction energies for the adsorption of Na<sup>+</sup>(H<sub>2</sub>O)<sub>n</sub> on Cu<sub>18</sub> are larger than those for Cu<sub>10</sub>, as could be expected from the results for the adsorption of a single Na<sup>+</sup> ion. The trends are the same, however: as *n* increases, Na<sup>+</sup> recedes from the surface and the interaction energy of the adsorbate and surface decreases.

Although there are no previous studies on the interactions between Na<sup>+</sup>(H<sub>2</sub>O)<sub>n</sub> and copper surfaces, our results for separately optimized Na<sup>+</sup>(H<sub>2</sub>O)<sub>n</sub> can be compared with similar results in the literature. When the various theoretical and experimental results are compared, it is useful to use incremental binding energies, which show how much the binding energy changes when the number of water molecules increases. The incremental binding energies of the Na<sup>+</sup>(H<sub>2</sub>O)<sub>n</sub> complex from this work and from the papers of Glendening and Feller,<sup>5</sup> Feller et al.,<sup>6</sup> Hashimoto and Morokuma,<sup>7</sup> Bauschlicher et al.,<sup>8</sup> and Džidić and Kebarle<sup>9</sup> are listed in Table 5. The method and basis set we used were the same as those used by Glendening and Feller<sup>5</sup> and Hashimoto and Morokuma<sup>7</sup> (MP2/6-31+G\*) with the exception that Hashimoto and Morokuma did not correct their results for BSSE. The results of Feller et al.<sup>6</sup> were also obtained with MP2 but this time with a more sophisticated correlation-consistent core/valence cc-pCVDZ basis set. Bauschlicher et al.<sup>8</sup> combined the MP2 method with a triple-ζ basis

**TABLE 4: MP2 Results for  $\text{Na}^+(\text{H}_2\text{O})_n\text{--Cu}_{18}$  Interaction**

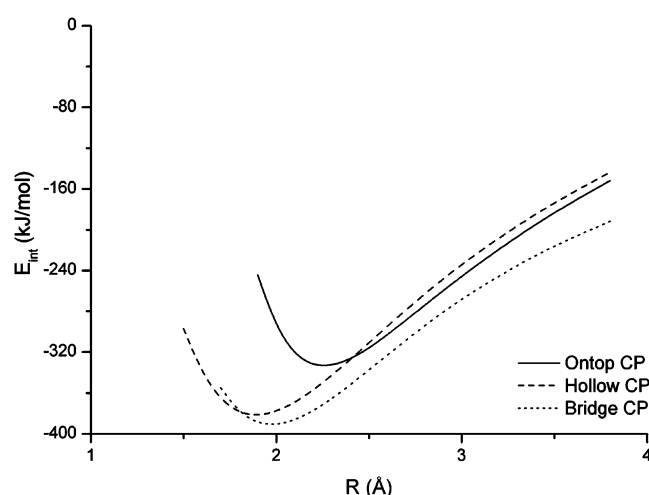
<i>n</i>	$R_{\text{eq}}$ (Å)	$E_{\text{tot}}$ <sup>b</sup> (au)	$E_{\text{comp}}$ <sup>c</sup> (au)	$E_{\text{int}}$ <sup>d</sup> (kJ/mol)	$E_{\text{tot}}$ CP <sup>e</sup> (au)	$E_{\text{comp}}$ CP <sup>e</sup> (au)	$E_{\text{int}}$ CP <sup>e</sup> (kJ/mol)	BSSE <sup>f</sup> (kJ/mol)
1	2.74	−3780.6426	−237.9099	−188.1	−3780.6268	−237.9067	−155.1	33.0
2	2.91	−3856.8795	−314.1572	−160.8	−3856.8575	−314.1493	−123.9	36.9
3	3.21	−3933.1131	−390.3979	−142.2	−3933.0853	−390.3867	−98.5	43.7

<sup>a</sup> Distance between  $\text{Na}^+$  and the Cu surface at the optimum geometry. <sup>b</sup> Total energy of the  $\text{Na}^+(\text{H}_2\text{O})_n\text{--Cu}_{18}$  system in hartrees. <sup>c</sup> Total energy of a separately optimized  $\text{Na}^+(\text{H}_2\text{O})_n$  complex in hartrees. <sup>d</sup> Interaction energy between  $\text{Cu}_{18}$  and the  $\text{Na}^+(\text{H}_2\text{O})_n$  complex obtained from the expression  $E_{\text{tot}} - (E_{\text{comp}} + E(\text{Cu}_{18}))$ , where  $E(\text{Cu}_{18}) = -3542.6610$  au. <sup>e</sup> CP-corrected values of  $E_{\text{tot}}$ ,  $E_{\text{comp}}$ , and  $E_{\text{int}}$ . <sup>f</sup> Difference between  $E_{\text{int}}$  and  $E_{\text{int}}$  CP.

**TABLE 5: Incremental Binding Energies for the  $\text{Na}^+(\text{H}_2\text{O})_n$  Complex (kJ/mol)<sup>a</sup>**

<i>n</i>	$\Delta E_{\text{int}}$ <sup>b</sup> MP2 CP	Glendening and Feller <sup>5</sup>	Feller et al. <sup>6</sup>	Hashimoto and Morokuma <sup>7</sup>	Bauschlicher et al. <sup>8</sup>	Džidić and Kebarle (exp.) <sup>9 c</sup>
1	−101.5	−101.7	−97.1	−110.0	−103.8	−100.4
2	−89.0	−88.7	−89.5	−101.3	−93.3	−82.8
3	−75.1	−75.3	−74.9	−83.7	−80.3	−66.1
4	−58.6	−58.6	−65.3	−70.7		−57.7
5	−41.2		−52.3			−51.5

<sup>a</sup> The rows show the increase in total binding energy of the  $\text{Na}^+(\text{H}_2\text{O})_n$  complex when a water molecule is added to the system. <sup>b</sup> Results from this study. <sup>c</sup> Values are enthalpies  $\Delta H$ .

**Figure 7.** CP-corrected MP2 interaction energy curves for the  $\text{Cu}^+\text{--Cu}_{10}$  interaction at the on-top, bridge, and hollow adsorption sites.

set augmented with two sets of polarization functions. The experimental results of Džidić and Kerbarle<sup>9</sup> were obtained by mass spectrometry. As expected, our results for the  $\text{Na}^+(\text{H}_2\text{O})_n$  complex are identical with the results of Glendening and Feller<sup>5</sup> because the methods were the same. Hashimoto and Morokuma used the same methods but did not account for the BSSE. However, our results before the CP correction are the same as theirs. Our results also correlate well with the those of Feller et al.<sup>6</sup> and Bauschlicher et al.<sup>8</sup> The experimental results of Džidić and Kerbarle differ from the theoretical results at some points, but we note that their values are enthalpies and they made no attempt to estimate the error limits of their experiments.

**3.3. Adsorption of  $\text{Cu}^+$ .** The interaction energy curves for the interaction of  $\text{Cu}^+$  and the smaller  $\text{Cu}_{10}$  cluster at the three main adsorption sites are presented in Figure 7. Several significant differences can be seen when the energy curves are compared with the  $\text{Na}^+\text{--Cu}_{10}$  interaction energy curves in Figure 2.  $\text{Cu}^+\text{--Cu}_{10}$  interaction energies are more than twice as large as the corresponding  $\text{Na}^+\text{--Cu}_{10}$  values, the equilibrium distances are much shorter, and the energy differences between the adsorption sites are substantial.  $\text{Cu}^+\text{--Cu}_{10}$  interaction energies were also calculated for the same 11 adsorption sites as for  $\text{Na}^+$ . The MP2 interaction energies and equilibrium distances are listed in Table 6. The results indicate that the most favorable adsorption site for  $\text{Cu}^+$  is the bridge site with a CP-corrected interaction energy of −392 kJ/mol. The interaction

**TABLE 6: MP2 Results for the  $\text{Cu}^+\text{--Cu}_{10}$  Interaction at 11 Adsorption Sites**

site	$R_{\text{eq}}$ <sup>a</sup> (Å)	$E_{\text{int}}$ <sup>b</sup> (kJ/mol)	$R_{\text{eq}}$ CP <sup>c</sup> (Å)	$E_{\text{int}}$ CP <sup>c</sup> (kJ/mol)	BSSE <sup>d</sup> (kJ/mol)	$\Delta E_{\text{int}}$ CP <sup>e</sup> (kJ/mol)
1	2.18	−396.6	2.25	−334.8	61.9	57.1
2	2.16	−405.3	2.22	−343.1	62.2	48.8
3	2.08	−420.6	2.15	−358.1	62.5	33.7
4	1.96	−441.0	2.04	−378.3	62.7	13.5
5	1.89	−452.2	1.97	−391.8	60.4	0.0
6	1.86	−445.8	1.93	−384.6	61.2	7.2
7	1.81	−443.3	1.88	−382.6	60.7	9.2
8	1.89	−441.2	1.97	−377.7	63.5	14.2
9	2.04	−420.9	2.11	−357.8	63.1	34.0
10	2.14	−404.4	2.21	−341.9	62.5	49.9
11	1.99	−431.7	2.05	−368.4	63.2	23.4

<sup>a</sup> Equilibrium distance between  $\text{Cu}^+$  and the Cu surface. <sup>b</sup> Interaction energy at the equilibrium distance. <sup>c</sup> CP-corrected values of  $R_{\text{eq}}$  and  $E_{\text{int}}$ . <sup>d</sup> Difference between  $E_{\text{int}}$  and  $E_{\text{int}}$  CP. <sup>e</sup> The relative CP-corrected interaction energy of the site when the energy of the most favorable adsorption site is set to zero.

energy at the hollow site is close to the value of the bridge site (difference 9.2 kJ/mol), while the on-top site is the least favorable adsorption site (difference to bridge site 57.1 kJ/mol). The potential energy surface is not flat as for  $\text{Na}^+\text{--Cu}_{10}$  interactions but has steep peaks at the on-top site, as can be seen from the potential energy map in Figure 8. The CP-corrected adsorbate–surface distances vary from 1.88 to 2.25 Å. The CP-corrected distance between the  $\text{Cu}^+$  adsorbate and nearest surface atom is 2.35 Å for the bridge site and 2.39 Å for the hollow site, both being a little shorter than the bulk Cu–Cu distance of 2.56 Å. This shortening of the distance can be attributed to the positive charge of the  $\text{Cu}^+$  adsorbate. Comparison of the interaction energies and equilibrium distances for  $\text{Na}^+$  and  $\text{Cu}^+$  adsorption shows that orbital interactions dominate the  $\text{Cu}^+\text{--Cu}_{10}$  interaction and that  $\text{Cu}^+$  is likely to adsorb on sites where it can bind to more than one surface atom.

The magnitude of the BSSE for the  $\text{Cu}^+\text{--Cu}_{10}$  interaction energies is 13–16% of the uncorrected energies, which is a little larger than the BSSE for the  $\text{Na}^+\text{--Cu}_{10}$  interaction. CP correction does not change the order of magnitude of the energetically most favored sites. The larger value of the BSSE for  $\text{Cu}^+\text{--Cu}_{10}$  than for  $\text{Na}^+\text{--Cu}_{10}$  interaction is a result of the more complex interactions between  $\text{Cu}^+$  and the copper surface. The more complex interactions also lead to a poorer performance of the uncorrected Hartree–Fock method. Relative to the CP-corrected MP2 results, the interaction energies obtained with HF are almost 30% smaller and the differences in equilibrium



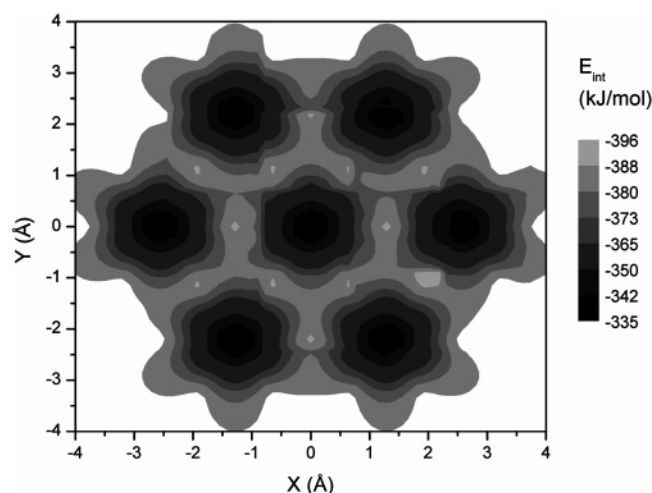


**Figure 8.** Potential energy surface for the interaction of  $\text{Cu}^+$  and  $\text{Cu}_{10}$ . Energy values are CP-corrected MP2 energies. The surface was created by plotting the adsorption energies in Table 6 against the set of points created by multiplying the points in Figure 3.

**TABLE 7: MP2 Results for the  $\text{Cu}^+ - \text{Cu}_{18}$  Interaction at Three Different Adsorption Sites**

site <sup>a</sup>	$R_{\text{eq}}^b$ (Å)	$E_{\text{int}}^c$ (kJ/mol)	$R_{\text{eq}}^{\text{CP}d}$ (Å)	$E_{\text{int}}^{\text{CP}d}$ (kJ/mol)	BSSE <sup>e</sup> (kJ/mol)	$\Delta E_{\text{int}}^{\text{CP}f}$ (kJ/mol)
on-top (1)	2.17	-460.9	2.24	-393.1	67.7	53.7
bridge (5)	1.87	-517.4	1.95	-435.6	81.9	11.2
hollow (7)	1.81	-530.3	1.89	-446.8	83.5	0.0

<sup>a</sup> Number after the adsorption site refers to the numbers used in Table 6. <sup>b</sup> Equilibrium distance between  $\text{Cu}^+$  and the Cu surface. <sup>c</sup> Interaction energy at the equilibrium distance. <sup>d</sup> CP-corrected values of  $R_{\text{eq}}$  and  $E_{\text{int}}$ . <sup>e</sup> Difference between  $E_{\text{int}}$  and  $E_{\text{int}}^{\text{CP}}$ . <sup>f</sup> Relative CP-corrected interaction energy of the site when the energy of the most favorable adsorption site is set to zero.

distances vary from 0.15 to 0.25 Å. However, the HF results are still qualitatively correct, with the bridge and hollow sites being energetically most favorable and the on-top site the least favorable.

We also examined the composition of interaction energies of  $\text{Na}^+$  and  $\text{Cu}^+$  on the surface of the  $\text{Cu}_{10}$  cluster with the Morokuma–Kitaura (MK) energy decomposition scheme.<sup>31</sup> MK analysis produced the correct interaction energies for both adsorbates, but the decomposition results were not consistent as the energy was composed of several very large terms canceling each other. The analysis produced negligible polarization and charge-transfer terms for  $\text{Na}^+$  when compared to  $\text{Cu}^+$ , which is in line with the notion that the  $\text{Cu}^+$ –surface interaction is more complex than the  $\text{Na}^+$ –surface interaction. According to the analysis, about one-third of the HF interaction energy results from electrostatic interactions. In addition to MK analysis, we carried out an alternative energy decomposition analysis with a reduced variational space (RVS) scheme<sup>32</sup> that obeys the Pauli exclusion principle. However, the results obtained with RVS were equally inconclusive.

For  $\text{Cu}^+$  and the larger  $\text{Cu}_{18}$  cluster, the interaction energies were calculated only for on-top, bridge, and hollow sites. The MP2 interaction energies and equilibrium distances are shown in Table 7. The hollow site had the largest CP-corrected interaction energy (-446.8 kJ/mol), but the difference with the bridge site was only 11.3 kJ/mol (<3% of the total interaction energy). Again the on-top site was the least favorable adsorption site, with 53.7 kJ/mol lower interaction energy than the hollow site. Comparison of the  $\text{Cu}^+ - \text{Cu}_{18}$  results with the results for the smaller cluster shows the CP-corrected interaction energies

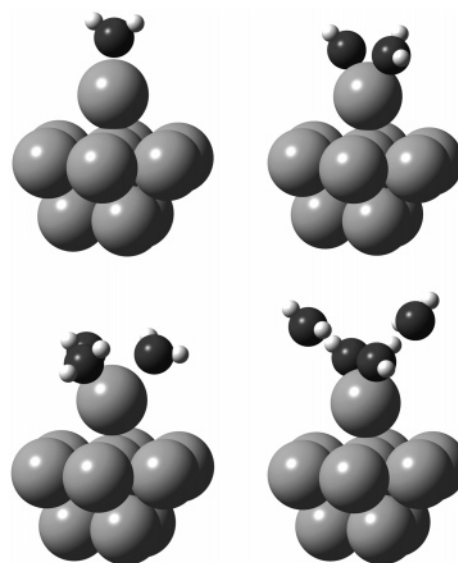


**Figure 9.** Optimized structures of the  $\text{Cu}^+(\text{H}_2\text{O})_n$  complex adsorbed on the  $\text{Cu}_{10}$  cluster for one to four water molecules.  $\text{Cu}^+$  was allowed to move only perpendicularly to the surface, but the water molecules were not restricted.  $\text{Cu}^+ - \text{H}_2\text{O}$  distances were 2.12 to 2.36 Å when  $n$  was 1–3, the distance increasing with the number of water molecules. When  $n$  was 4, the two closest water molecules were at a distance of 2.23 Å from  $\text{Cu}^+$  and the two other molecules were at a distance of 3.60 Å.

for  $\text{Cu}^+ - \text{Cu}_{18}$  to be 10–20% larger but the equilibrium distances are practically the same. The results for the  $\text{Cu}^+ - \text{Cu}_{18}$  interaction are consistent with the conclusion that the orbital interactions dominate the interaction between  $\text{Cu}^+$  and the copper surface and  $\text{Cu}^+$  prefers sites where it can bind to more than one surface atom.

Jacob et al.<sup>4</sup> studied the adsorption of the Cu atom on the Cu(111) surface using embedded and nonembedded copper clusters. Their primary interest was to develop embedding methods, and large nonembedded clusters were used as a reference. The largest nonembedded cluster was one consisting of 98 Cu atoms in five layers built up from 32, 25, 24, 13, and 4 Cu atoms. With the B88/P86 density functional, the interaction energy was -172.7 kJ/mol for the adsorption of a Cu atom on a Cu(100) surface described with a  $\text{Cu}_{98}$  cluster. The equilibrium distance was 3.34 Å, which is almost double our value for hollow and bridge sites of the (111) surface. Their interaction energy is about 40% of our CP-corrected MP2 energy for the adsorption of  $\text{Cu}^+$  on the hollow site of the  $\text{Cu}_{18}$  cluster. This difference and the large distance between the Cu atom and the Cu surface indicate that the interactions between the Cu atom and the Cu surface are not nearly as strong as those between  $\text{Cu}^+$  and the Cu surface.

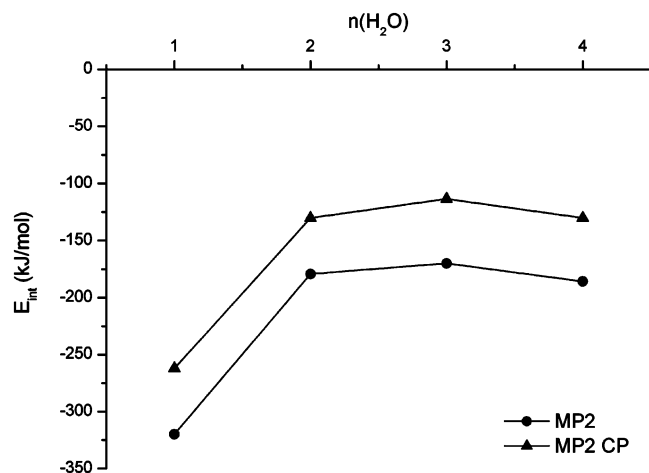
**3.4. Adsorption of  $\text{Cu}^+(\text{H}_2\text{O})_n$ .** The adsorption of the  $\text{Cu}^+(\text{H}_2\text{O})_n$  complexes on the  $\text{Cu}_{10}$  cluster was investigated with one to four water molecules, and the approach to the problem was identical with the treatment of the  $\text{Na}^+(\text{H}_2\text{O})_n$  complex. Structures were optimized with HF, and the same geometrical restrictions were laid on  $\text{Cu}^+$  as on  $\text{Na}^+$ . The final adsorbate geometries (Figure 9) show that even when the number of water molecules around  $\text{Cu}^+$  increases,  $\text{Cu}^+$  is not drawn away from the surface as  $\text{Na}^+$  is, but instead the water molecules begin to form a hydrogen bond network with one another. The MP2 energies for the adsorption of  $\text{Cu}^+(\text{H}_2\text{O})_n$  are shown in Table 8.

The values of  $E_{\text{int}}$  and  $E_{\text{int}}^{\text{CP}}$  in Table 8 indicate that the interaction energy between the  $\text{Cu}^+(\text{H}_2\text{O})_n$  complex and  $\text{Cu}_{10}$

**TABLE 8: MP2 Results for the  $\text{Cu}^+(\text{H}_2\text{O})_n\text{--Cu}_{10}$  Interaction**

$n$	$R_{\text{eq}}$ (Å)	$E_{\text{tot}}^b$ (au)	$E_{\text{comp}}^c$ (au)	$E_{\text{int}}^d$ (kJ/mol)	$E_{\text{tot}}^e$ CP <sup>e</sup> (au)	$E_{\text{comp}}^e$ CP <sup>e</sup> (au)	$E_{\text{int}}^e$ CP <sup>e</sup> (kJ/mol)	BSSE <sup>f</sup> (kJ/mol)
1	2.44	−2240.8451	−272.7299	−319.8	−2240.8158	−272.7225	−262.1	57.6
2	2.52	−2317.0734	−349.0116	−179.3	−2317.0377	−348.9946	−130.2	49.1
3	2.59	−2393.3025	−425.2443	−170.0	−2393.2599	−425.2232	−113.5	56.5
4	2.55	−2469.5392	−501.4748	−186.1	−2469.4925	−501.4493	−130.7	55.4

<sup>a</sup> Distance between  $\text{Cu}^+$  and the Cu surface at the optimum geometry. <sup>b</sup> Total energy of the  $\text{Cu}^+(\text{H}_2\text{O})_n\text{--Cu}_{10}$  system in hartrees. <sup>c</sup> Total energy of a separately optimized  $\text{Cu}^+(\text{H}_2\text{O})_n$  complex in hartrees. <sup>d</sup> Interaction energy between  $\text{Cu}_{10}$  and the  $\text{Cu}^+(\text{H}_2\text{O})_n$  complex obtained from the expression  $E_{\text{tot}} - (E_{\text{comp}} + E(\text{Cu}_{10}))$ , where  $E(\text{Cu}_{10}) = -1967.9935$  au. <sup>e</sup> CP-corrected values of  $E_{\text{tot}}$ ,  $E_{\text{comp}}$ , and  $E_{\text{int}}$ . <sup>f</sup> Difference between  $E_{\text{int}}$  and  $E_{\text{int}}$  CP.

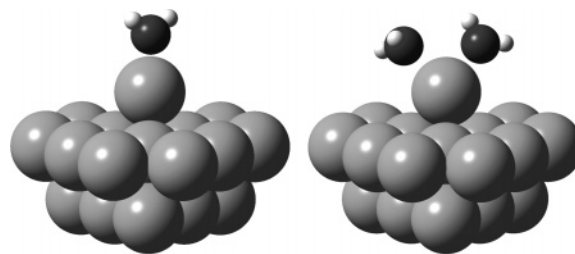
**Figure 10.** MP2 interaction energy and CP-corrected interaction energy between the  $\text{Cu}^+(\text{H}_2\text{O})_n$  complex and  $\text{Cu}_{10}$  cluster.

cluster decreases as the number of water molecules increases from one to three. When  $n$  increases to 4, the water molecules form a hydrogen bond network with one another and only two water molecules bind directly to  $\text{Cu}^+$ . Since the waters form hydrogen bonds with each other instead of binding to  $\text{Cu}^+$ ,  $\text{Cu}^+$  can interact better with the surface and  $E_{\text{int}}$  CP increases. The change in the interaction energy is illustrated in Figure 10. From the geometry optimizations and interaction energies of the  $\text{Cu}^+(\text{H}_2\text{O})_n$  complex on  $\text{Cu}_{10}$  cluster, it would seem that in aqueous solution  $\text{Cu}^+$  will prefer to adsorb directly on the surface instead of having additional water molecules surrounding it. This is opposite of the behavior of  $\text{Na}^+$ , which becomes surrounded by water molecules and recedes from the surface as  $n$  increases.

HF could not exactly reproduce the qualitative trend seen in Figure 10 as it showed a slight decrease instead of increase in  $E_{\text{int}}$  when  $n$  increased to 4. This result can probably be explained in terms of a failure of HF to describe the energetics of the hydrogen bonds.

With the larger  $\text{Cu}_{18}$  cluster, the geometry optimizations were performed without any geometrical restrictions on  $\text{Cu}^+$ . Only cases with one and two water molecules were examined as the optimizations were time-consuming. The final adsorbate geometries for  $\text{Cu}^+(\text{H}_2\text{O})_n$  optimizations on  $\text{Cu}_{18}$  are shown in Figure 11, and the corresponding MP2 energies are listed in Table 9. The interaction energies for the adsorption of  $\text{Cu}^+(\text{H}_2\text{O})_n$  on  $\text{Cu}_{18}$  are larger than those for  $\text{Cu}_{10}$ , as could be expected from the results for the adsorption of a single  $\text{Cu}^+$  ion.  $\text{Cu}^+$  recedes only 0.06 Å from the surface as the number of water molecules increases from one to two, which is in line with the results obtained with the smaller cluster.

As with the  $\text{Na}^+(\text{H}_2\text{O})_n$  complex, there are no previous studies on the interactions between  $\text{Cu}^+(\text{H}_2\text{O})_n$  and copper surfaces. Thus, only the results for separately optimized  $\text{Cu}^+(\text{H}_2\text{O})_n$  can be compared with results in the literature. Again, the notion of incremental binding energy is used to compare the various theoretical and experimental results. The incremental binding

**Figure 11.** Optimized structures of the  $\text{Cu}^+(\text{H}_2\text{O})_n$  complex adsorbed on the  $\text{Cu}_{18}$  cluster for one and two water molecules. The complex was allowed to move freely on the surface.  $\text{Cu}^+\text{--H}_2\text{O}$  distances were 2.13–2.35 Å, the distance increasing with the number of water molecules.

energies of the  $\text{Cu}^+(\text{H}_2\text{O})_n$  complex from this work and from the works of Feller et al.,<sup>10</sup> Bauschlicher et al.,<sup>11</sup> and several mass spectrometry groups<sup>12–14</sup> are listed in Table 10. Feller et al. used two different sets of methods, one exactly the same as used in this study and the other a set of very large basis sets and high-level methods designed to achieve a complete basis set (CBS) estimate of binding energies. The CBS estimates were obtained with CCSD(T). Where  $n = 3$  and 4, however, their CBS results are for structures where some water molecules are bound to other water molecules and not to  $\text{Cu}^+$ . Our results are for complexes where all water molecules are bound to  $\text{Cu}^+$ , and thus, the second set of results from Feller et al. (column 4 in Table 10) shows their best estimates of the incremental energies for such complexes. Bauschlicher et al. combined the MCPF method with a double- $\zeta$  basis set augmented with one set of polarization functions. The experimental results were obtained by mass spectrometry. All theoretical and experimental studies show the incremental binding energy of the second water molecule to be larger than the binding energy of the first water molecule, and additional water molecules have substantially smaller binding energies.

**3.5. Effect of the Cluster Size.** Since the adsorption energies obtained for  $\text{Cu}_{10}$  and  $\text{Cu}_{18}$  are somewhat different in size, we decided to investigate how the adsorption energies change when the size of the cluster increases. HF on-top interaction energies for  $\text{Na}^+$  at the distance of 2.7 Å were calculated with four larger cluster models:  $\text{Cu}_{22}$ ,  $\text{Cu}_{38}$ ,  $\text{Cu}_{46}$ , and  $\text{Cu}_{82}$ . The variation of interaction energy is shown in Figure 12. The interaction energy oscillates and does not converge straightforwardly as the cluster size increases. This phenomenon, potentially arising from the finite size of the cluster, is sometimes exhibited by transition metal clusters.<sup>25,27</sup> An example of the oscillating behavior of adsorption energies on copper surfaces was recently seen in the study by Dominguez-Ariza et al.<sup>30</sup> They used 10 different-sized cluster models to study the effect of the surface model on the chemisorption of atomic hydrogen on  $\text{Cu}(001)$ . None of the used computational methods (HF, MP2, B3LYP, and GGA-PW91) could produce a converging series of adsorption energies. However, even if the absolute binding energy might be sensitive to the cluster size, other properties reflecting the character of the bond, such as bonding mechanism and adsorption sites, have



**TABLE 9: MP2 Results for Cu<sup>+</sup>(H<sub>2</sub>O)<sub>n</sub>–Cu<sub>18</sub> Interaction**

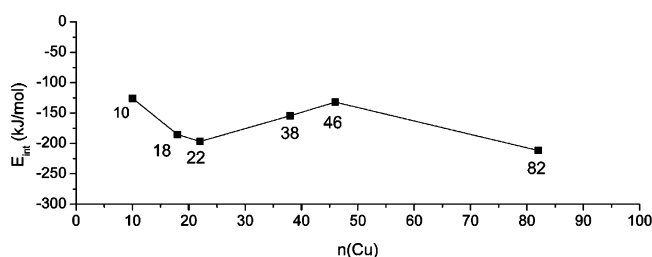
<i>n</i>	<i>R</i> <sub>eq</sub> (Å)	<i>E</i> <sub>tot</sub> <sup>b</sup> (au)	<i>E</i> <sub>comp</sub> <sup>c</sup> (au)	<i>E</i> <sub>int</sub> <sup>d</sup> (kJ/mol)	<i>E</i> <sub>tot</sub> CP <sup>e</sup> (au)	<i>E</i> <sub>comp</sub> CP <sup>e</sup> (au)	<i>E</i> <sub>int</sub> CP <sup>e</sup> (kJ/mol)	BSSE <sup>f</sup> (kJ/mol)
1	2.16	−3815.5546	−272.7299	−429.9	−3815.5175	−272.7225	−351.8	78.2
2	2.22	−3891.7833	−349.0116	−290.6	−3891.7374	−348.9946	−214.7	75.8

<sup>a</sup> Distance between Cu<sup>+</sup> and the Cu surface at the optimum geometry. <sup>b</sup> Total energy of the Cu<sup>+</sup>(H<sub>2</sub>O)<sub>n</sub>–Cu<sub>18</sub> system in hartrees. <sup>c</sup> Total energy of a separately optimized Cu<sup>+</sup>(H<sub>2</sub>O)<sub>n</sub> complex in hartrees. <sup>d</sup> Interaction energy between Cu<sub>18</sub> and the Cu<sup>+</sup>(H<sub>2</sub>O)<sub>n</sub> complex obtained from the expression *E*<sub>tot</sub> − (*E*<sub>comp</sub> + *E*(Cu<sub>18</sub>)), where *E*(Cu<sub>18</sub>) = −3542.6610 au. <sup>e</sup> CP-corrected values of *E*<sub>tot</sub>, *E*<sub>comp</sub>, and *E*<sub>int</sub>. <sup>f</sup> Difference between *E*<sub>int</sub> and *E*<sub>int</sub> CP.

**TABLE 10: Incremental Binding Energies for the Cu<sup>+</sup>(H<sub>2</sub>O)<sub>n</sub> Complex (kJ/mol)<sup>a</sup>**

<i>n</i>	Δ <i>E</i> <sub>int</sub> <sup>b</sup> MP2 CP	Feller et al. CCSD(T) CBS <sup>10</sup>	Feller et al. CCSD(T)/ MP2 <sup>10 c</sup>	Bauschlicher et al. <sup>11</sup>	Holland and Castleman (exp.) <sup>12</sup>	Magnera et al. (exp.) <sup>13</sup>	Dalleska et al. (exp.) <sup>14 d</sup>
1	−160.3	−161.1	−161.1	−162.3		−146 ± 12.6	−161 ± 5.9
2	−166.4	−174.1	−174.1	−164.8		−163 ± 12.6	−170 ± 6.7
3	−51.9	−76.1 <sup>e</sup>	−61.9	−64.4	−66.1 ± 0.8	−71 ± 8.4	−57 ± 7.5
4	−45.5	−69.5 <sup>f</sup>	−38.5	−55.6	−67.4 ± 0.8	−63 ± 8.4	−54 ± 4.2

<sup>a</sup> Each row shows the increase in total binding energy of the Cu<sup>+</sup>(H<sub>2</sub>O)<sub>n</sub> complex when a water molecule is added to the system. <sup>b</sup> Results from this study. <sup>c</sup> The best estimate of Feller et al. for complexes with all water molecules bound to Cu<sup>+</sup>. All energies were obtained with CCSD(T) or MP2 and high-level basis sets. <sup>d</sup> Values are enthalpies Δ*H*. <sup>e</sup> The actual configuration of water molecules was 2 + 1, which means that one water molecule was bound to another water molecule and not to Cu<sup>+</sup>. <sup>f</sup> The configuration of water molecules was 2 + 2.

**Figure 12.** HF interaction energies for Na<sup>+</sup> at the on-top site of different-sized Cu clusters. The distance between Na<sup>+</sup> and the surface was 2.7 Å.

been found to vary little with cluster size.<sup>33</sup> With our cluster models, hundreds of atoms might be required before the quantitatively correct interaction energy is obtained, but the size of the cluster does not affect the relative trends, such as the different behavior of Na<sup>+</sup> and Cu<sup>+</sup> with and without water molecules.

#### 4. Conclusions

The adsorption of Na<sup>+</sup>, Na<sup>+</sup>(H<sub>2</sub>O)<sub>n</sub>, Cu<sup>+</sup>, and Cu<sup>+</sup>(H<sub>2</sub>O)<sub>n</sub> on the copper (111) surface described with Cu<sub>10</sub> and Cu<sub>18</sub> cluster models was studied by an ab initio MP2 method. The 6-31+G\* basis set was used for water and sodium and a split valence RECP with 19 active electrons for copper. BSSE was taken into account by applying the counterpoise correction. The interactions between Na<sup>+</sup> and the copper surface were found to be primarily electrostatic and the energy differences among the adsorption sites were small. The electrostatic nature of the Na<sup>+</sup>–Cu interaction results in Na<sup>+</sup> having no preference for adsorption on the surface if the alternative is to be completely surrounded by water molecules. This was clearly seen in the adsorption studies on the Na<sup>+</sup>(H<sub>2</sub>O)<sub>n</sub> complex where Na<sup>+</sup> receded from the Cu surface as water molecules were added to the system and finally became totally surrounded by them.

In contrast to the electrostatic interactions between Na<sup>+</sup> and the Cu surface, Cu<sup>+</sup>–Cu interactions were dominated by orbital interactions. Cu<sup>+</sup> prefers to adsorb on sites where it can bind to more than one surface atom, and the interactions are much stronger than the Na<sup>+</sup>–Cu interactions. The significance of the orbital interactions was evident in the adsorption studies on the Cu<sup>+</sup>(H<sub>2</sub>O)<sub>n</sub> complex where Cu<sup>+</sup>, unlike Na<sup>+</sup>, was not drawn away from the surface, but instead the water molecules began to form hydrogen bonds with one another. As an overall result,

we conclude that in an aqueous solution Cu<sup>+</sup> will attach to metallic copper surface and Na<sup>+</sup> will stay in solution.

The larger cluster model used in this work, Cu<sub>18</sub>, was superior to the smaller Cu<sub>10</sub> cluster in many ways. The discrepancies between Hartree–Fock and MP2 were smaller with the larger model, and the structural optimizations of the adsorbates could be performed without any artificial geometrical restrictions. Unfortunately, extensive use of the Cu<sub>18</sub> cluster was prohibited by the large cost of calculations that included the Cu<sub>18</sub> cluster and additional adsorbate molecules. The absolute interaction energies obtained with Cu<sub>10</sub> and Cu<sub>18</sub> are different, and calculations with even larger clusters (up to Cu<sub>82</sub>) revealed that the convergence of the interaction energies is not straightforward as the cluster size increases. However, the relative trends, such as the different behavior of Na<sup>+</sup> and Cu<sup>+</sup> with and without water molecules, were not affected by the cluster size.

HF was able to describe the electrostatic interactions of Na<sup>+</sup> with the copper surface almost as well as MP2, but the description of the Na<sup>+</sup>(H<sub>2</sub>O)<sub>n</sub> complex became less quantitative when the number of water molecules increased. In the case of Cu<sup>+</sup> and the Cu<sup>+</sup>(H<sub>2</sub>O)<sub>n</sub> complex, the performance of HF was only qualitative when compared with MP2. The magnitude of BSSE was substantial in most cases, and taking it into account with the counterpoise method was important. CP corrections did not, however, have a significant impact on the relative trends among the interaction energies.

**Acknowledgment.** Funding from the Academy of Finland is gratefully acknowledged. Dr. Henna Ruuska provided useful information and data in the early phases of this work.

#### References and Notes

- (1) Jakubke, H.-D.; Jeschkeit H. In *Concise Encyclopedia Chemistry*, 1st ed.; Wiley: New York, 1993; pp 263–265.
- (2) Bunshah, R. F. In *Handbook of Deposition Technologies For Films and Coatings*, 2nd ed.; Noyes Publications: Park Ridge, NJ, 1994; p 23.
- (3) Padilla-Campos, A.; Toro-Labbe, A.; Maruani, A. *Surf. Sci.* **1997**, 385 (1), 24.
- (4) Jacob, T.; Anton, J.; Sarpe-Tudoran, C.; Sepp, W.-D.; Fricke, B.; Bastug, T. *Surf. Sci.* **2003**, 536 (1–3), 45.
- (5) Glendening, E. D.; Feller, D. *J. Phys. Chem.* **1995**, 99, 3060.
- (6) Feller, D.; Glendening, E. D.; Woon, D. E.; Feyereisen, M. W. *J. Chem. Phys.* **1995**, 103 (9), 3526.
- (7) Hashimoto, K.; Morokuma, K. *J. Am. Chem. Soc.* **1994**, 116, 11436.
- (8) Bauschlicher, C. W., Jr.; Langhoff, S. R.; Partridge, H. *J. Chem. Phys.* **1991**, 95, 5142.
- (9) Džidić, I.; Kebarle, P. *J. Phys. Chem.* **1970**, 74, 1466.

- (10) Feller, D.; Glendening, E. D.; de Jong, W. A. *J. Chem. Phys.* **1999**, *110* (3), 1475.
- (11) Bauschlicher, C. W., Jr.; Langhoff, S. R.; Partridge, H. *J. Chem. Phys.* **1991**, *94*, 2068.
- (12) Holland, P. M.; Castleman, A. W., Jr. *J. Chem. Phys.* **1982**, *76*, 4195.
- (13) Magnera, T. F.; David, D. E.; Stulik, D.; Orth, R. G.; Jonkman, H. T.; Michl, J. *J. Am. Chem. Soc.* **1989**, *111*, 5036.
- (14) Dalleska, N. F.; Honma, K.; Sunderlin, L. S.; Armentrout, P. B. *J. Am. Chem. Soc.* **1994**, *116*, 3519.
- (15) Ruuska, H.; Pakkanen, T. A.; Rowley, R. *J. Phys. Chem. B* **2004**, *108*, 2614.
- (16) Sauer, J.; Ugliengo, P.; Garrone, E.; Saunders, V. R. *Chem. Rev.* **1994**, *94*, 2095.
- (17) Boys, S. F.; Bernardi, F. *Mol. Phys.* **1970**, *19*, 553.
- (18) Feller, D. *J. Chem. Phys.* **1992**, *96*, 6104.
- (19) Masamura, M. *Theor. Chem. Acc.* **2001**, *106*, 301.
- (20) Dolg, M.; Wedig, U.; Stoll, H.; Preuss, H. *J. Chem. Phys.* **1987**, *96*, 6796.
- (21) Basis sets were obtained from the Extensible Computational Chemistry Environment Basis Set Database, Version 10/21/03, as developed and distributed by the Molecular Science Computing Facility, Environmental and Molecular Sciences Laboratory which is part of the Pacific Northwest Laboratory, P.O. Box 999, Richland, WA 99352 and funded by the U.S. Department of Energy. The Pacific Northwest Laboratory is a multiprogram laboratory operated by Battelle Memorial Institute for the U.S. Department of Energy under Contract DE-AC06-76RLO 1830. Contact David Feller or Karen Schuchardt for further information.
- (22) Frisch, M. J.; Trucks, G. W.; Schlegel, H. B.; Scuseria, G. E.; Robb, M. A.; Cheeseman, J. R.; Montgomery, J. A., Jr.; Vreven, T.; Kudin, K. N.; Burant, J. C.; Millam, J. M.; Iyengar, S. S.; Tomasi, J.; Barone, V.; Mennucci, B.; Cossi, M.; Scalmani, G.; Rega, N.; Petersson, G. A.; Nakatsuji, H.; Hada, M.; Ehara, M.; Toyota, K.; Fukuda, R.; Hasegawa, J.; Ishida, M.; Nakajima, T.; Honda, Y.; Kitao, O.; Nakai, H.; Klene, M.; Li, X.; Knox, J. E.; Hratchian, H. P.; Cross, J. B.; Bakken, V.; Adamo, C.; Jaramillo, J.; Gomperts, R.; Stratmann, R. E.; Yazyev, O.; Austin, A. J.; Cammi, R.; Pomelli, C.; Ochterski, J. W.; Ayala, P. Y.; Morokuma, K.; Voth, G. A.; Salvador, P.; Dannenberg, J. J.; Zakrzewski, V. G.; Dapprich, S.; Daniels, A. D.; Strain, M. C.; Farkas, O.; Malick, D. K.; Rabuck, A. D.; Raghavachari, K.; Foresman, J. B.; Ortiz, J. V.; Cui, Q.; Baboul, A. G.; Clifford, S.; Cioslowski, J.; Stefanov, B. B.; Liu, G.; Liashenko, A.; Piskorz, P.; Komaromi, I.; Martin, R. L.; Fox, D. J.; Keith, T.; Al-Laham, M. A.; Peng, C. Y.; Nanayakkara, A.; Challacombe, M.; Gill, P. M. W.; Johnson, B.; Chen, W.; Wong, M. W.; Gonzalez, C.; Pople, J. A. *Gaussian 03*, Revision B.01; Gaussian, Inc.: Wallingford, CT, 2004.
- (23) Ahlrichs, R.; Bär, M.; Häser, M.; Horn, H.; Kölmel, C. *Chem. Phys. Lett.* **1989**, *162*, 165 (b) Häser, M.; Ahlrichs, R. *J. Comput. Chem.* **1989**, *10*, 104 (c) Horn, H.; Weiss, H.; Häser, M.; Ehrig, M.; Ahlrichs, R. *J. Comput. Chem.* **1991**, *12*, 1058.
- (24) Schmidt, M. W.; Baldridge, K. K.; Boatz, J. A.; Elbert, S. T.; Gordon, M. S.; Jensen, J. H.; Koseki, S.; Matsunaga, N.; Nguyen, K. A.; Su, S.; Windus, T. L.; Dupuis, M.; Montgomery, J. A., Jr. *J. Comput. Chem.* **1993**, *14*, 1347.
- (25) Whitten, J. L.; Yang, H. *Surf. Sci. Rep.* **1996**, *24*, p 65.
- (26) Bagus, P. S.; Illas, F. In *Encyclopedia of Computational Chemistry*; Wiley: New York, 1998; Vol 4, p 2870.
- (27) Minot, C.; Markovits, A. *THEOCHEM* **1998**, *424*, 119.
- (28) Borg, R. J.; Dienes, G. J. In *The Physical Chemistry of Solids*, 1st ed.; Academic Press: San Diego, CA, 1992; p 23.
- (29) Hoffmann, R. In *Solids and Surfaces: A Chemist's View of Bonding in Extended Structures*, 1st ed.; VCH Publishers: New York, 1988; p 22.
- (30) Dominguez-Ariza, D.; Sousa, C.; Harrison, N. M.; Ganduglia-Pirovano, M. V.; Illas, F. *Surf. Sci.* **2003**, *522*, 185.
- (31) Morokuma, K. *J. Chem. Phys.* **1971**, *35*, 1236. (b) Kitaura, K.; Morokuma, K. *Int. J. Quantum Chem.* **1976**, *10*, 325.
- (32) Stevens, W. J.; Fink, W. H. *Chem. Phys. Lett.* **1987**, *139*, 15.
- (33) ref 25, p 74.